Iwona Sulima, Marta Homa, Piotr Malczewski

High-temperature corrosion resistance of steel-matrix composites

Wysokotemperaturowa odporność korozyjna kompozytów stalowych

Abstract

The results of corrosion studies of composite materials obtained by two methods of powder metallurgy are presented in the article. The main goal of the studies was to determine the high-temperature corrosion resistance of steel-matrix composites reinforced with 8 vol.% TiB_2. Thermogravimetric analyses were conducted at 1100°C in air during a 24 h cycle. The microstructure of the composite after thermogravimetric studies was observed with a scanning electron microscope.

Keywords: composite, austenitic stainless steel, Differential Thermal Analysis (DTA), Thermogravimetric Analysis (TG)

Streszczenie

Praca prezentuje wyniki badań korozyjnych materiałów kompozytowych otrzymanych dwoma metodami metalurgii proszków (PM). Głównym celem pracy było określenie wysokotemperaturowej odporności korozyjnej kompozytów o osnowie stali austenitycznej umacnianych 8% obj. TiB_2. Przeprowadzono badania termograwimetryczne w temperaturze 1100°C w atmosferze powietrza w cyklu 24-godzinnym. Mikrostrukturę powierzchni kompozytów po badaniach termograwimetrycznych obserwowano przy użyciu skaningowej mikroskopii elektronowej.

Słowa kluczowe: kompozyt, stal austenityczna, termiczna analiza różnicowa (DTA), termograwimetria (TG)

1. Introduction

Thermal analysis is applied in metallurgy to determine the physicochemical properties of metals and alloys as well as metal-matrix composites [1–3]. Thermal analysis allows us

Iwona Sulima Ph.D. Eng., Piotr Malczewski Ph.D. Eng.: Institute of Technology, Pedagogical University of Cracow, Krakow, Poland, **Marta Homa Ph.D. Eng.:** Center for High-Temperature Studies, Foundry Research Institute, Krakow, Poland; isulima@up.krakow.pl

to describe features of the material as functions of time and temperature. Under the influence of temperature changes (heating and cooling), specific heat of materials change and, moreover, materials may undergo physical (e.g., melting, boiling, evaporation, crystallization, sublimation) or chemical (e.g., oxidation, reduction) transformations. Taking advantage of the possibilities given by thermal analysis, mass loss, water content, temperatures of physical transformations, thermal effects of exothermic and endothermic reaction, thermal effects associated with physical changes and chemical reactions, thermodynamic parameters such as enthalpy, entropy or specific heat can be determined. The mentioned data allows us to determine comprehensively technological properties and chose parameters of technological processes when the studied materials are used [4–7]. Thermogravimetry allows us to measure changes of mass (loss or gain) with changes of temperature or time. In a TG curve, steps connected with mass loss or gain of the sample during its heating or cooling can be observed. Differential thermogravimetric curves (DTG) present the change of reaction rate of a substance with an increase or decrease in temperature or as a function of time [6, 8]. Differential thermal analysis (DTA) registers differences of temperature (ΔT) between a studied sample and a reference sample, which are placed in identical conditions in heated or cooled environments. Temperatures of both samples are usually measured by means of thermocouples that are connected differentially. The result of the analysis is the characteristics of difference in voltage between sample and reference thermocouples with respect to temperature. When the temperature of the studied material is higher than that of the reference sample, this means that an exothermic reaction occurs. On the other hand, an endothermic reaction takes place when the temperature of the studied material is lower than the temperature of the reference sample [7, 8].

The corrosion properties of the sintered austenitic stainless steels were studied using electrochemical methods in aggressive media. The producing methods and treatment significantly influences the corrosive properties of the steel [9]. Hamdy et al. [10] observed a marked increase in corrosion resistance of nitrided stainless steel even after maintaining two weeks in an NaCl solution. Effects of the treatment temperature was also studied. It was shown that those as-polished samples nitrided at 450°C have the highest corrosion resistance. Padmavathi et al. [11] observed that microwave sintering of 316L steel at supersolidus temperature (1400°C) resulted in improved corrosion resistance as compared to solid state and conventional sintered samples.

Furthermore, the corrosion resistance of austenitic steel sintered with boron is discussed in detail [12–14]. Besides, in order to improve the corrosion resistance, the effects of copper, tin, and other additions to steel powder were the subjects of investigations in [15–17]. Also, another method of corrosion-resistance improvement is the introduction of ceramic particles to steel [18, 19]. For example, Padmavathi et al. [20] investigated the corrosion resistance of the 316Lsteel composites with 5 and 10 wt.% YAG in an H_2SO_4 solution. The superior corrosion resistance and higher passivation behavior were received

for composites with 5 wt.% YAG (at 1400°C). This is mainly due to microstructural coarsening, homogeneous melt distribution along the grain boundaries, and removal of almost all pores. The literature on the corrosion behavior of austenitic steel composites with borides is very limited. There are no published reports on the corrosion behavior of steel composites with borides sintered by the HP-HT and SPS methods.

Steel-matrix composites with ceramic particulates have significant potential for structural applications due to their high specific strength and stiffness [21–23]. The incorporation of ceramic particulates into the steel-matrix can improve hardness, strength, and wear resistance. Corrosion behavior is a very important parameter for assessing the application potential of composites as structural materials. However, the corrosion resistance of steel-matrix composites is always inferior to their monolithic matrix alloys due to one or more of following possible reasons: (1) galvanic coupling of the reinforcement constituent and matrix; (2) the formation of an interfacial phase between the matrix and reinforcement; and (3) microstructural changes and processing contaminants resulting from the manufacture of the steel-matrix composite [24, 25].

The aim of this paper is to analyze the corrosion resistance of steel-matrix composites reinforced with TiB_2 at a high temperature (1100°C).

2. Methods

The commercial AISI 316L austenitic stainless steel (particle size of about 25 μm, Hoganas), TiB_2 (particle size of 2.5–3.5 μm, H.C. Starck), and boron (particle size of 5–7 μm, Goodfellows) powders were employed as starting materials. The mixing of the steel and ceramic powders was carried out in a Turbula mixer for 8 hours. A few options of composites reinforced with 8 vol.% TiB_2 (steel + 8% TiB_2) were sintered. In the case of some of them, boron in an amount of 1 vol.% was added to the austenitic-steel matrix (final composition: steel + 8% TiB_2 + 1% B). The composites were obtained by one of two modern techniques: High Pressure – High Temperature (HP-HT) and Spark Plasma Sintering (SPS). Tables 1 and 2 presents the conditions of sintering the composites. In the case of the HP-HT method, the powders of the mixtures were formed into discs (15 mm in diameter, 5 mm in height) by pressing a steel matrix under a pressure of 200 MPa. The sintering process was conducted using a Bridgman-type apparatus. The SPS process was carried out using an HPD 5 FCT System GmbH furnace. Powders are compacted in a graphite die using a maximum pressure of 35 MPa in a vacuum. Next, the SPS furnace chamber introduced argon, which acted as a protective gas. Details regarding the applied sintering methods and properties of the studied composites are given in [26, 27].

Thermogravimetric analyses were carried out with NETZCH equipment with an STA 449 F3 Jupiter attachment coupled with mass spectrometer QMS 403C Aëolos (Fig. 1). The device can be applied to perform TG-DSC/DTA measurements of a wide array of materials, including ceramics, metals, alloys, chemical compounds, polymers,

composites, etc. A compensation technique in a scale mechanism allows us to perform mass-change measurements of the analyzed sample with an accuracy of 1 μg in the range of mass change 0–35 mg. In addition, the unique construction of the protective gas flow eliminates the risk of damage to the scale mechanism by evaporating reaction gases.

Table 1. The HP-HT sintering conditions of composites used in corrosion studies

Composite	Sintering method	Temperature [°C]	Pressure [GPa]
Steel + 8% TiB$_2$	HP-HT	1300	7
Steel + 8% TiB$_2$ + 1% B	HP-HT	1300	7

Table 2. The SPS Sintering conditions of composites used in corrosion studies

Composite	Sintering method	Temperature [°C]	Time [min]
Steel + 8% TiB$_2$	SPS	1100	5
Steel + 8% TiB$_2$	SPS	1100	30
Steel + 8% TiB$_2$ + 1% B	SPS	1100	5
Steel + 8% TiB$_2$ + 1% B	SPS	1100	30

a)

b)
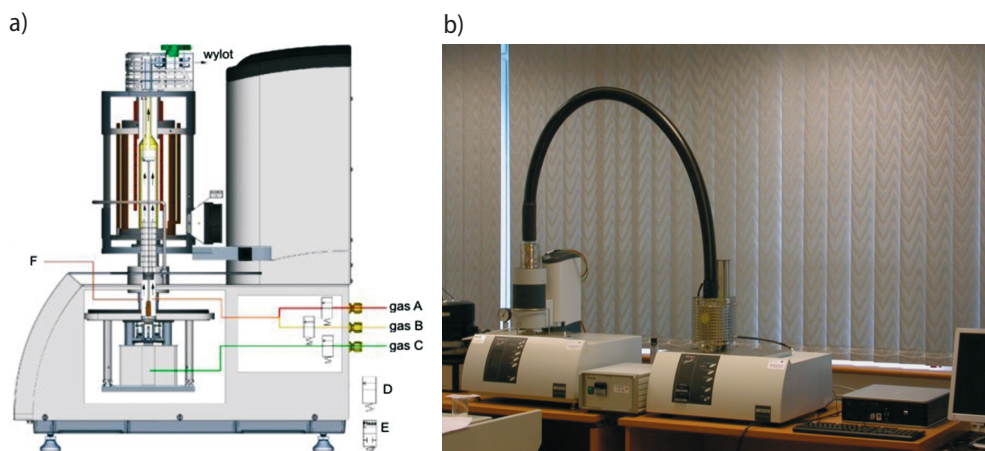
Fig. 1. a) Schematic diagram of STA 449 F3 Jupiter Netzsch thermal analyzer; b) apparatus type STA 449 F3 Jupiter with QMS 403C Aëolos mass spectrometer, which was used in tests TG-DSC/DTA [28]

As a part of our high-temperature corrosion studies, measurements of mass changes as a function of time (24 h) TG/DTA at 1100°C in air were conducted. The microstructure of the sintered materials before and after the corrosion experiments was characterized by scanning electron microscopy (JEOL JSM 6610LV) with an EDS (Energy Dispersive Spectroscopy) detector.

3. Results and discussion

In Figures 2–7, dependencies of mass change from temperature (TG) and DTA for the studied composites are presented. Thermal analysis showed an increase of mass with time (24 h) at a constant temperature of 1100°C. It can be suspected that, in an air atmosphere, an oxidation process of the composites takes place at the surface. Analysis of TG data (Figs 2–4) proves that the total mass gain after 24 hours reaches the following levels: 8.56 mg, 12.79 mg and 8.29 mg for steel + 8% TiB$_2$ composites sintered at 1300°C-7 GPa (HP-HT), 1100°C-5 min (SPS) and 1100°C-30 min (SPS), respectively.

In the case of the given materials, the DTA curve does not show any peaks characteristic of phase transition at the mentioned ranges of time and temperature. In 24 hours of testing, the increment of mass is uniform for the discussed composites (Figs 2–4).

Besides, an increase of mass was also observed in the case of samples made of steel + 8% TiB$_2$ + 1% B after 24 hours (TG curves, Figs 5–7). The total increase of mass for materials sintered at 1300°C-7 GPa (HP-HT) is established at a level of 7.98 mg. In the case of composites reinforced with boron (Fig. 5), the total increase of mass is less than that of the unmodified composites (Fig. 2). One strong stage of gaining mass is observed at the TG curve after 4 h (Fig. 5). The analyzed composites exhibit some changes in the DTA curves in the form of a single exothermic effect after 3.5 h of test duration. In the remaining part of the test (which lasted up to 24 h), the monotony of the DTA curve has not been altered.
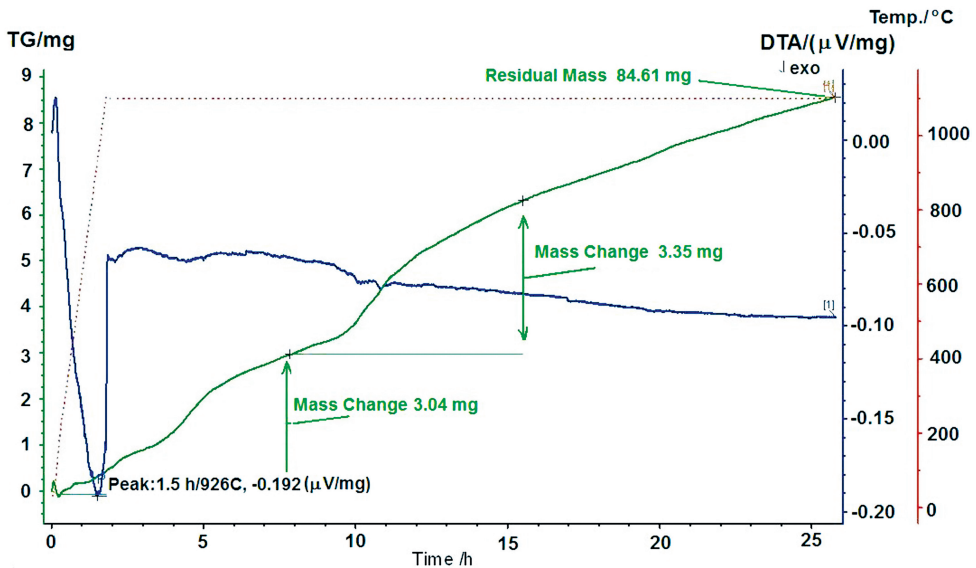

Fig. 2. Relationships between changes in mass and temperature (TG) and differential thermal analysis (DTA) for steel + 8% TiB$_2$ composite (HP-HT sintering, 1300°C-7 GPa)
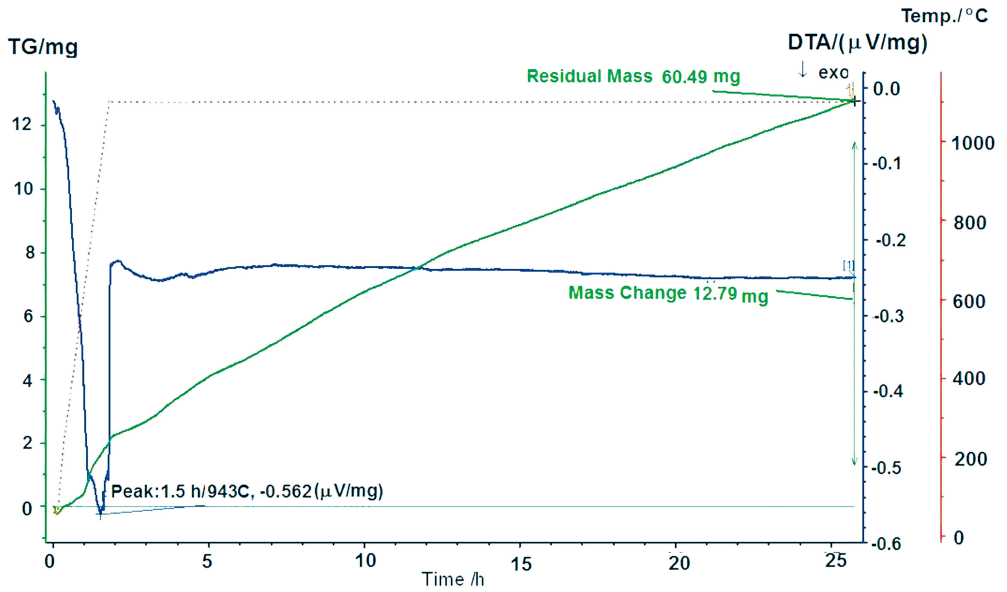
Fig. 3. Relationships between changes in mass and temperature (TG) and differential thermal analysis (DTA) for steel + 8% TiB$_2$ composite (SPS process, 1100°C-5 min)
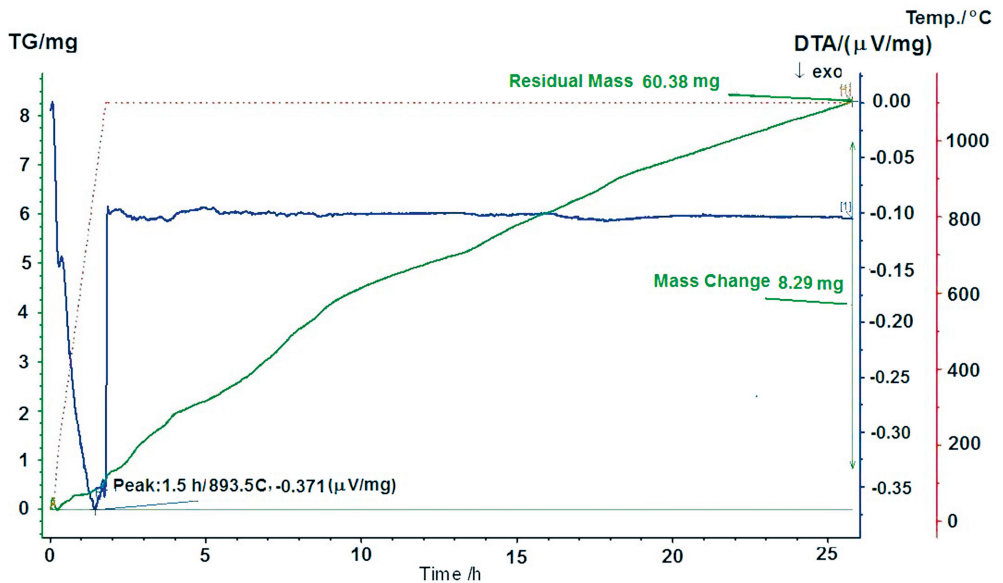

Fig. 4. Relationships between changes in mass and temperature (TG) and differential thermal analysis (DTA) for steel + 8% TiB$_2$ composite (SPS process, 1100°C-30 min)
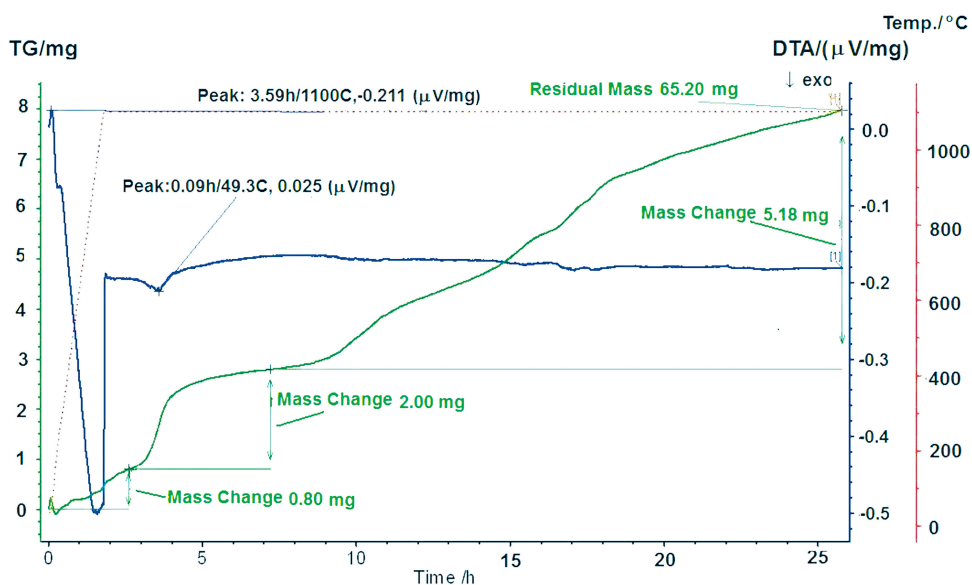
Fig. 5. Relationships between changes in mass and temperature (TG) and differential thermal analysis (DTA) for steel + 8% TiB₂ + 1%B composite (HP-HT sintering, 1300°C-7 GPa)

On the other hand, in the case of the same composites sintered by the SPS method at 1100°C-5 min (Fig. 6), the total increase of mass is 9.94 mg. Also, the composites modified with boron (Fig. 6) show a smaller total mass gain compared to the unmodified composites (Fig. 3). In the TG curve, two distinct stages of increasing mass occurring for different periods of time and with various rates are observed after testing times of 2.5 and 6 h; later, the mass gain took place quite uniformly. Characteristic peaks indicating phase transitions were also observed. The minima of the peaks prove an exothermic reaction at the given time and temperature of 1100°C, which is associated with heat absorption or emission. The two observed exothermic effects of DTA characteristics happened after testing times of about 2.5 and 6 hours. The remaining testing times (up to 24 h) did not affect the monotony of the DTA curve.

An exception consists in composites modified with boron and obtained by the SPS method in conditions of 1100°C-30 min. These materials showed a higher mass gain (10.08 mg, Fig. 7) as compared to steel + 8% TiB₂ composites (8.29 mg, Fig. 4). Besides, it is observed that steel + 8% TiB₂ + 1% B composites sintered at 1100°C-30 min (SPS) exhibit a quite-uniform increase of mass during the 24 hours of testing. The conditions of conducting the test did not influence the change of monotony of the DTA curve in 24 hours. Analysis of the DTA curves does not show the presence of any peaks, which could indicate an endothermic or exothermic reaction.
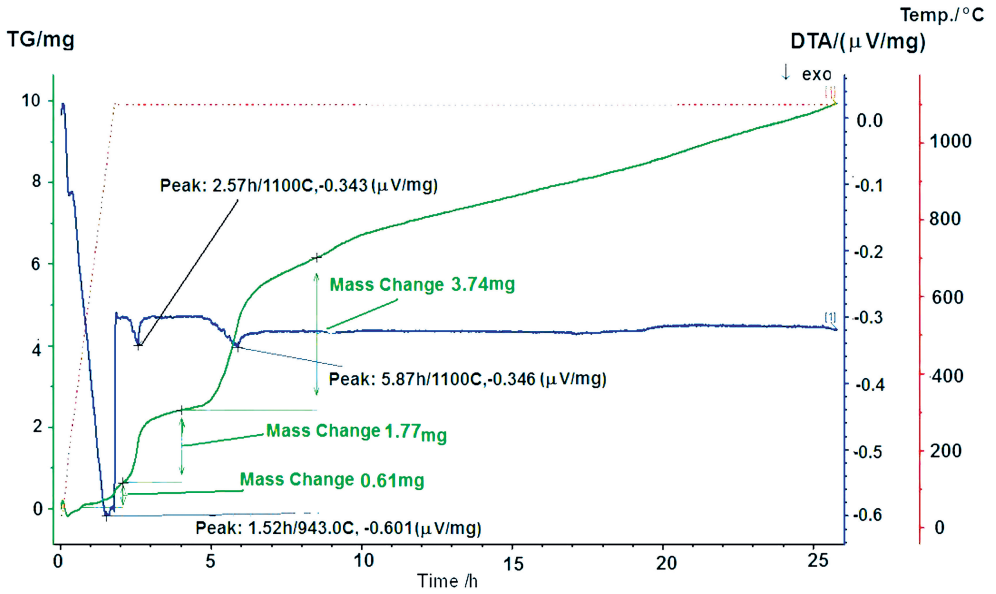
Fig. 6. Relationships between changes in mass and temperature (TG) and differential thermal analysis (DTA) for steel + 8% TiB$_2$ + 1% B composite (SPS process, 1100°C-5 min)
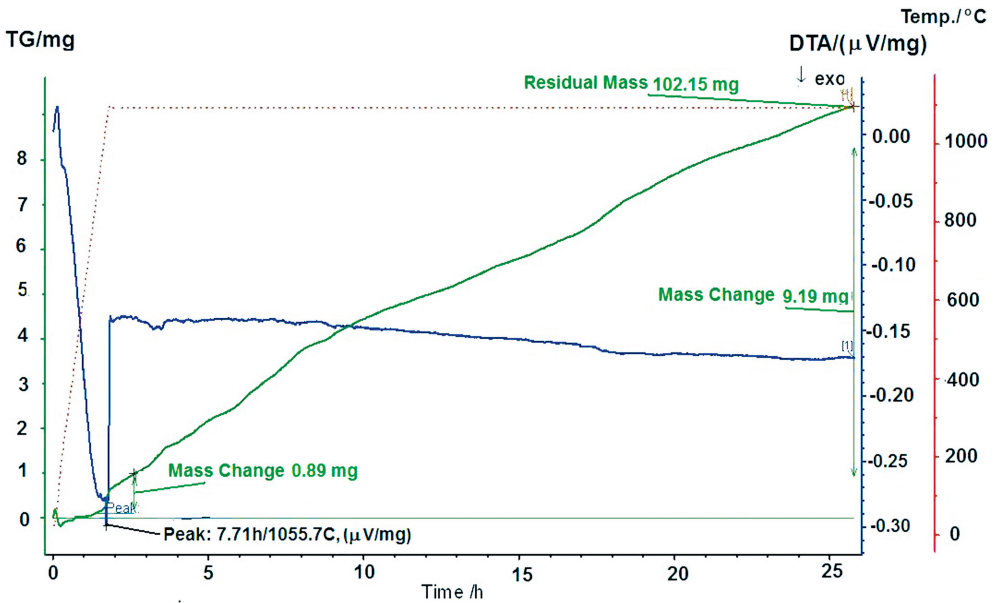

Fig. 7. Relationships between changes in mass and temperature (TG) and differential thermal analysis (DTA) for steel + 8% TiB$_2$ + 1% B composite (SPS process, 1100°C-30 min)

Microstructural observations of the composite surfaces before and after thermogravimetric studies were carried out. Typical microstructures of the sintered composites before testing are presented in Figure 8. An SEM observation showed that all composites had a uniform dispersion of fine TiB_2 particles (dark precipitates) in the austenitic steel-matrix. The reinforcing TiB_2 phase had the tendency to settle along the steel-matrix grain boundaries. Differences were revealed in the microstructure of materials sintered by SPS as compared to the materials sintered by the HP-HT method. Application of the SPS method promotes the formation of new phases. Chemical analysis of composites sintered by SPS disclosed the presence of numerous precipitates in the microstructure, containing mainly chromium [29].

a)

b)

c)

d)
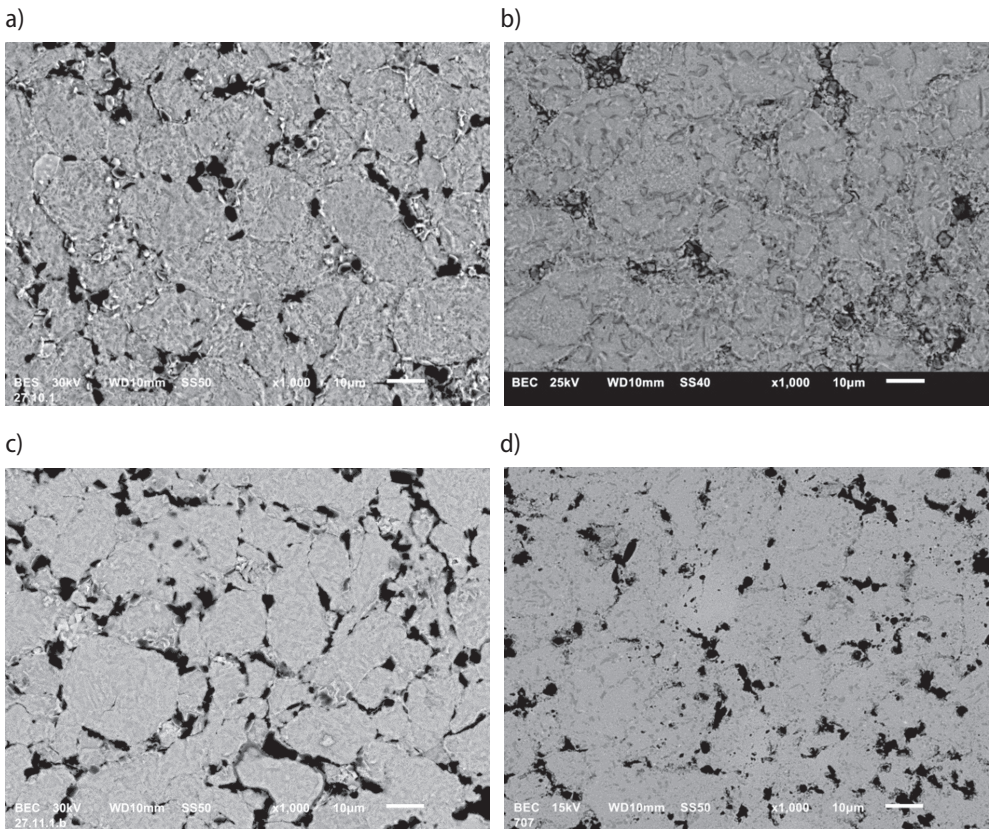
Fig. 8. SEM micrograph of the steel-8% TiB_2 composite sintered at: a) 1300°C-7 GPa (HP-HT);
b) 1100°C-30 min (SPS); and the steel + 8% TiB_2 + 1% B composite sintered at: c) 1300°C-7 GPa (HP-HT);
d) 1100°C-30 min (SPS)

Surface morphology of the composites after corrosion experiments is presented in Figures 9–11. The surfaces of all composites show the formation of a characteristic oxide layer when the corrosion studies were carried out in air. According to literature [30, 31],

three iron oxides may be formed at the surface of steel-matrix composites such as Fe_2O_3, Fe_3O_4, and FeO phases, which directly adhere to the composite surface. Moreover, it was found that, at high temperatures above 800°C, chromium oxide (Cr_2O_3) and complex oxides such as $FeCr_2O_4$ or $(Fe, Ni, Cr)O_4$ can be formed on the steel surface [17, 32, 33].

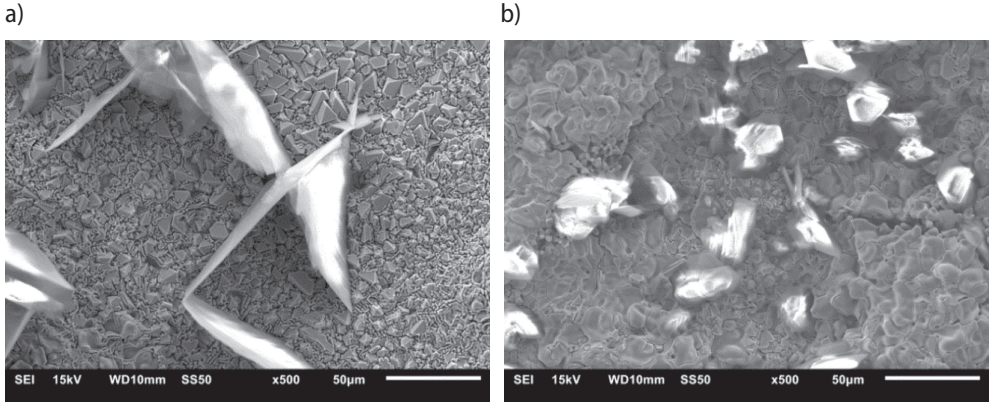a)   b)

Fig. 9 Microstructure (SEM) of the surface of composites after tests for: a) steel-8% TiB$_2$ composite (HP-HT process, 1300°C-7 GPa); b) steel + 8% TiB$_2$ + 1% B composite (HP-HT process, 1300°C-7 GPa)

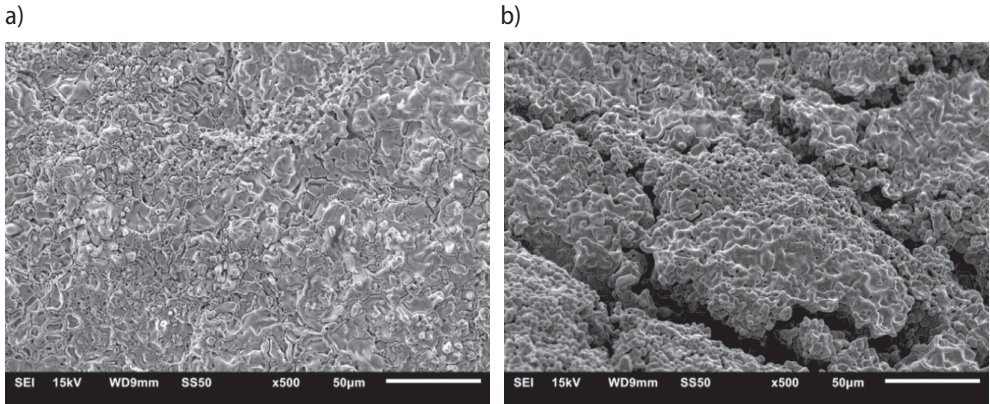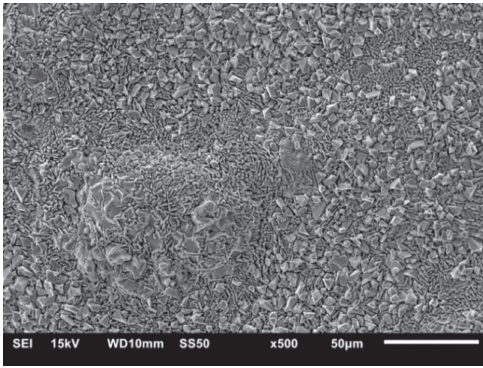a)   b)

Fig. 10. Microstructure (SEM) of the surface of composites after tests for: a) steel + 8% TiB$_2$ composite (SPS process, 1100°C-5 min); b) steel + 8% TiB$_2$ composite (SPS process, 1100°C-30 min)

It was observed for all composites, that the oxide layers are not uniform as they contain local cracks (Figs 10b and 11b). The observed layers show different morphology. In the case of composites sintered by the SPS method in a temperature of 1100°C, oxides are observed in the form of fine crystallites with well-developed lateral surfaces (e.g., Fig. 11a).
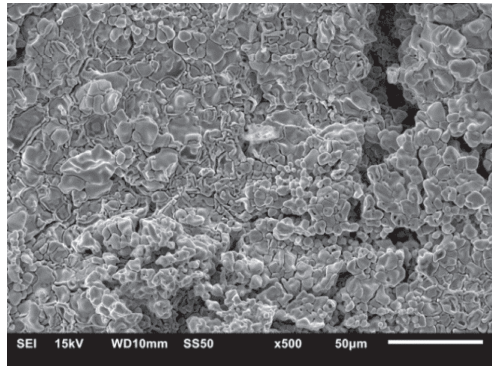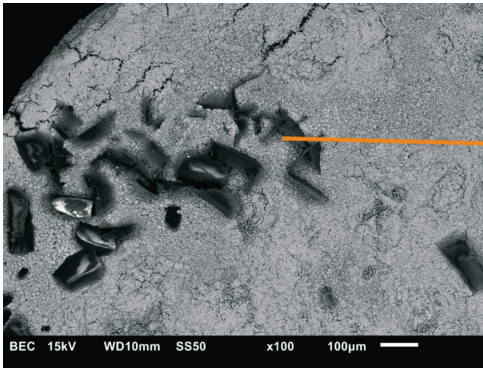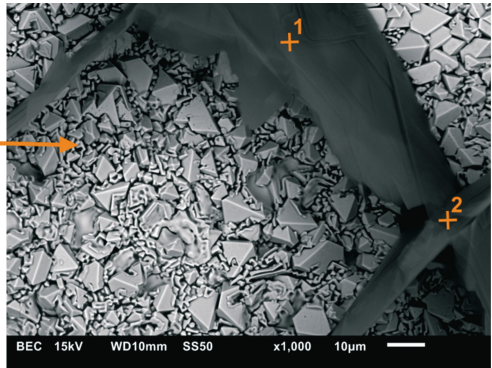
a)

b)

Fig. 11. Microstructure (SEM) of the surface of composites after tests for: a) steel + 8% TiB$_2$ + 1% B composite (SPS process, 1100°C-5 min); b) steel + 8% TiB$_2$ + 1% B composite (SPS process, 1100°C-30 min)
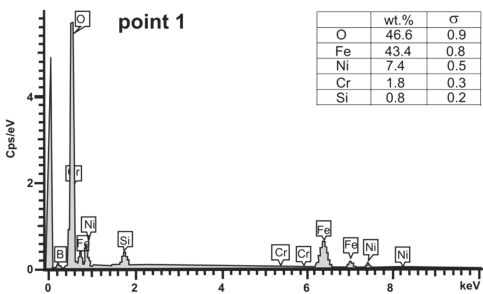
a)

b)

c)

d)

point 1	wt.%	σ
O	46.6	0.9
Fe	43.4	0.8
Ni	7.4	0.5
Cr	1.8	0.3
Si	0.8	0.2

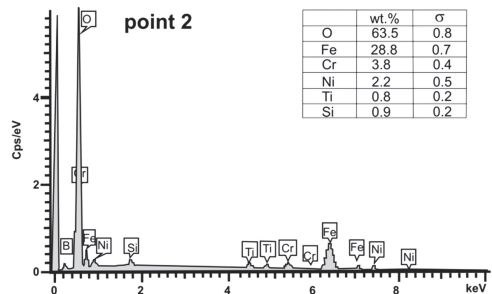| point 2	wt.%	σ
O	63.5	0.8
Fe	28.8	0.7
Cr	3.8	0.4
Ni	2.2	0.5
Ti	0.8	0.2
Si	0.9	0.2

Fig. 12. (a–b) microstructure (SEM) of the surface of composites after tests for steel+8%TiB$_2$ composite (HP-HT process, 1300°C-7 GPa); (c–d) EDS of point analysis

81

On the other hand, the oxide layers have a more-developed spongy form with cracks in composites sintered by the SPS method for 30 min (Figs 10b, 11b). The characteristic feature in composites sintered with the HP-HT method is the formation of additional iron oxides with a shape of comparatively large flakes emerging above normal oxide layer (steel-8%TiB$_2$ composite, Fig. 9a). In the case of composite steel-8% TiB$_2$-1%B, finer flakes of the oxide phase are observed. EDS analysis (Figs 12, 13) of the chemical composition of the phases confirm that flakes are indeed iron oxides. However, proper identification of the form requires a more-precise chemical analysis (which is planned to be done in the next stage of our studies).
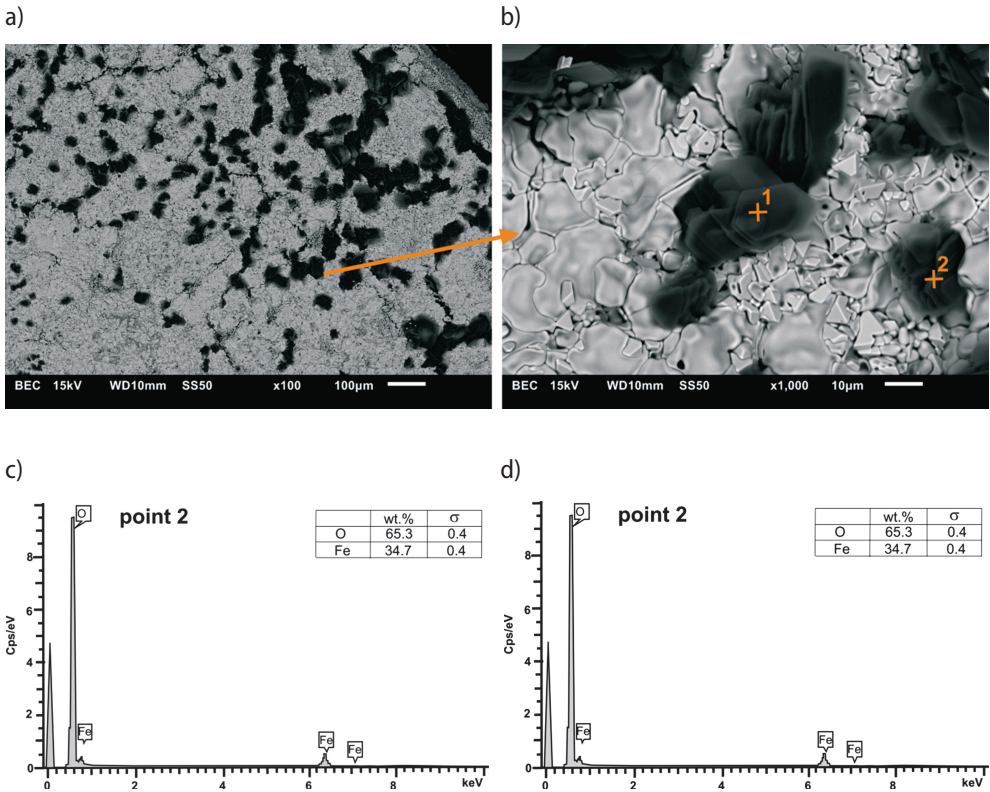

Fig. 13. (a–b) microstructure (SEM) of the surface of composites after tests for steel + 8% TiB$_2$ + 1% B composite (HP-HT process, 1300°C-7 GPa); (c–d) EDS of point analysis

4. Conclusions

The conducted thermal analysis showed an increase of mass as a function of time at a constant temperature of 1100°C for all of the studied composite materials. This indicates oxidation of the composite surface during experiments conducted in air. A different

mass gain with respect to the applied sintering method and conditions of the sintering process was observed. In the case of composites sintered by the SPS method, a DTA curve exhibited peaks characteristic of exothermic reactions.

Microstructural observations showed the formation of an oxide layer on the surface of the composites characterized by different morphology with local cracks.

Acknowledgements

References

 [1] Yu D., Zhu M., Utigard T.A., Barati M.: TG/DTA study on the carbon monoxide and graphite thermal reduction of a high-grade iron nickel oxide residue with the presence of siliceous gangue. Thermochimica Acta, 575, 10 (2014), 1–11

 [2] Jagdfeld H.-J., Odoj R.: A new high-temperature coupling system for TG/DTA-MS. Thermochimica Acta, 72, 1–2 (1984), 171–177

 [3] Matos M., Castanho J.M., Vieira M.T.: Composite copper/stainless steel coated powders. Journal of Alloys and Compounds, 483, 1–2 (2009), 460–463

 [4] Brown M.E.: Introduction to thermal analysis: techniques and applications. Chapman and Hall Ltd., London, 1988

 [5] Schultze D.: Termiczna analiza różnicowa. PWN, Warszawa, 1974

 [6] Szczepaniak W.: Metody instrumentalne w analizie chemicznej. PWN, Warszawa, 2002

 [7] Małecki A.: Wpływ różnych czynników na wyniki pomiarów DTA. I Szkoła Analizy Termicznej, Zakopane, 1996

 [8] Balcerowiak W.: Różnicowa kalorymetria skaningowa i termograwimetria – aspekty teoretyczne i praktyczne. V Szkoła Analizy Termicznej, Zakopane, 2008

 [9] Fredriksson W., Petrini D., Edström K., Björefors F., Nyholm L.: Corrosion resistances and passivation of powder metallurgical and conventionally cast 316L and 2205 stainless steels. Corrosion Science, 67 (2013), 268–280

[10] Hamdy A.S., Marx B., Butt D.: Corrosion behavior of nitride layer obtained on AISI 316L stainless steel via simple direct nitridation route at low temperature. Materials Chemistry and Physics, 126 (2011), 507–514

[11] Padmavathi C., Upadhyaya A., Agrawal D.: Corrosion behavior of microwave-sintered austenitic stainless steel composites. Scripta Materialia, 57 (2007), 651–654

[12] Kazior T., Karwan-Baczewska J., Banaś J.: The influence of sintering atmosphere on corrosion resistance of sintered austenitic stainless steel. Metalurgia Proszków, 3–4 (1993), 70–86

[13] Menapace C., Molinari A., Kazior J., Pieczonka T.: Surface self-densification in boron alloyed austenitic stainless steel and impact resistance. Powder Metallurgy, 50 (2007), 326–335

[14] Menapace C., Molinari A., Kazior J., Pieczonka T.: Surface phenomena on boron alloyed Astaloy CrM powders. Euro PM2007 Conference Proceedings, Toulouse (France), 1 (2007), 41–46

[15] Chatarjee S.K., Warwick M.E., Maykuth D.J.: The Effect of Tin, Copper, Nickel and Molybdenum on the Mechanical Properties and Corrosion Resistance of Sintered Stainless Steel (AISI 304L). Modern Developments in Powder Metallurgy, 16 (1985), 277–293

[16] Molinari A., Tesi B., Tiziani A., Feddrizzi L., Straffelini G.: Composition, Microstructure and Mechanical Property Relations in Sintered Stainless Steels. International Journal of Powder Metallurgy, 27, 1 (1991), 15–21

[17] Stavrev D.S., Dikova D., Ivanov I.P.: High-temperature gas corrosion of austenitic Cr-Ni steel containing Mo and Ti. Metal Science and Heat Treatment, 53, 9–10 (2012), 508–511

[18] Xu P., Lin Ch.X., Zhou Ch.Y., Yi X.P.: Wear and corrosion resistance of laser cladding AISI 304 stainless steel/Al_2O_3 composite coatings. Surface & Coatings Technology, 238 (2014), 9–14

[19] Trueman A.R., Schweinsberg D.P., Hope G.A.: The effect of chromium additions on the corrosion behaviour of tungsten carbide\carbon steel metal matrix composites. Corrosion Science, 40, 10 (1998), 1685–1696

[20] Padmavathi C., Panda S.S., Agarwal D., Upadhyaya A.: Effect of Microstructural Characteristics on Corrosion Behaviour of Microwave Sintered Stainless Steel Composites. Innovative Processing and Synthesis of Ceramics, Glasses and Composites, Organized by N.P. Bansal and J.P. Singh, Materials Science and Technology, MS&T 2006, 517–528

[21] Ni Z.F., Sun Y.S., Xue F., Bai J., Lu Y.J.: Microstructure and properties of austenitic stainless steel reinforced with in situ TiC particulate. Materials and Design, 32 (2011), 1462–1467

[22] Abenojar J., Velasco F., Bautista A., Campos M., Bas J.A., Torralba J.M.: Atmosphere influence in sintering process of stainless steels matrix composites reinforced with hard particles. Composites Science and Technology, 63 (2003), 69–79

[23] Sulima I., Klimczyk P., Malczewski P.: Effect of TiB_2 particles on the tribological properties of stainless steel matrix composites. Acta Metallurgica Sinica (English Letter), 27, 1 (2014), 12–18

[24] Hihara L.H.: Metal matrix composites. In: R. Baboian (ed.): Corrosion Tests and Standards. Second ed. PA: ASTM; MNL 20, Philadelphia, 2005, 637–655

[25] Bakkar A., Ata S.: Corrosion behaviour of stainless steel fibre-reinforced copper metal matrix composite with reference to electrochemical response of its constituents. Corrosion Science, 85 (2014), 343–351

[26] Sulima I., Jaworska L., Figiel P.: Influence of processing parameters and different content of TiB_2 ceramics on the properties of composites sintered by high temperature – high pressure (HT-HP) method. Archives of Metallurgy and Materials, 59, 1 (2014), 203–207

[27] Sulima I., Figiel P., Kurtyka P.: Austenitic stainless steel-TiB_2 composites obtained by HP-HT method. Composites Theory and Practice, 12, 4 (2012), 245–250

[28] Homa M., Siewiorek A.: Wykorzystanie metody TG oraz SPM w badaniach wysokotemperaturowego utleniania. In: N. Sobczak, M. Homa (red.), Małopolskie Centrum Innowacyjnych Technologii i Materiałów. Nowe możliwości badawcze Instytutu Odlewnictwa, Kraków 2011, 155–173

[29] Sulima I.: Consolidation of AISI316L Austenitic Steel – TiB_2 Composites by SPS and HP-HT Technology. In: Arunachalam Lakshmanan (ed.): Sintering Techniques of Materials, Rijeka, InTech- Open Access Publisher; 1 April 2015, 125–153

[30] Mrowec S.: Kinetyka i mechanizm utleniania metali. Wydawnictwo Śląsk, Katowice, 1982

[31] Łukaszczyk A., Pisarek M., Rożniatowski K., Banaś J.: Spektroskopowe badania powierzchniowych warstw anodowych otrzymanych na niskochromowych stopach Fe-Cr w 0,1 M roztworze Na_2SO_4. Ochrona przed Korozją, 3 (2012), 150–163

[32] Wang C.J., Li C.C.: The High-Temperature Corrosion of Austenitic Stainless Steel with a NaCl Deposit at 850°C. Oxidation of Metals, 61, 5–6 (2004), 485–505

[33] Shariff N.A., Jalar A., Sahri M.I., Othman N.K.: Effect of High Temperature Corrosion on Austenitic Stainless Steel Grade 304 in CO_2 Gas at 700°C. Sains Malaysiana, 43, 7 (2014), 1069–1075